Research article

Spectroscopic investigation on shuttlecock-shaped liquid crystalline trimers: Mesomorphic behaviour and its application in optical storage devices

D. Sandhya Kumari [a], Apoorva Shetty [b,c], B.S. Ranjitha [a], Vandana M [b,c], G. Shanker [a,*], Mohamed Alaasar [d], Gurumurthy Hegde [c,**]

[a] Department of Chemistry, Jnana Bharathi Campus, Bangalore University, Bengaluru, 560056, India
[b] Department of Chemistry, Christ University, Hosur Road, Bengaluru, 560029, India
[c] Centre for Advanced Research and Development (CARD), Christ University, Hosur Road, Bengaluru, 560029, India
[d] Department of Chemistry, Faculty of Science, Cairo University, Giza, Egypt

A B S T R A C T

In this paper, we discuss the synthesis and characterization of 2,3,4-tris[n-((4-(-cyanophenyl)diazenyl)phenoxy)alkyloxy]benzonitrile obtained by coupling 2,3,4-trihydroxy benzonitrile and (E)-4-((4-((n-bromoalkyl)oxy)phenyl)diazenyl)benzonitrile, pertain to shuttlecock shaped liquid crystals. The molecular structure was confirmed by NMR spectroscopic and elemental analyzer. The thermal behavior of the trimers was assessed using a polarizing optical microscope (POM) and differential scanning calorimetry (DSC). The three diazo groups in the trimers enabled us to study the photo-isomerization effect and evaluate their potential applications in optical storage devices. Importantly, we found these trimers easy to synthesize and process, paving the way for cost-effective alternatives to traditional LC materials. We fabricated an optical storage device to study the light effects on shuttlecock-shaped LC trimers, demonstrating that the geometry of the trimers plays a crucial role in determining structure-property relationships.

1. Introduction

Smart materials are envisioned to be the integral part of next generation of advanced devices and digitally augmented technologies [1]. Liquid crystal (LC) is one such material, where in the dual combination of order and mobility are explored in piezoelectric, chromactive, magnetorheological, photoactive device applications [2]. Although, the LCs in the display technology emerged as one of the best material to date, additionally their material properties are investigated for other applications in optoelectronics like light-emitting diodes (LED), photovoltaics, optical fibres, laser diodes, photoresistors and more in the coming days [3–6]. The chromophores and the overall shape of the molecule on their self-assembly lead to the formation of interesting material properties [7–10]. The nonconventional molecular design approach has significantly enhanced the advanced liquid crystalline properties, offering a wider range of contrasting features compared to traditional rod and disc-shaped molecules [11–18]. The presence of azo functional moieties displays unique optoelectronic properties mainly due to thermally stable photoisomerization and their fatigue resistance [19–21]. Light induced molecular shape distortion are added advantage for surface adsorption phenomena which could be explored in the storage device [22,23]. Azo-based liquid crystals with room temperature mesomorphic properties are significant for their potential applications in flexible displays, optical devices, and biomedical sensors, contributing to advancements in electronics and photonics

---

* Corresponding author.
** Corresponding author.
E-mail addresses: maanshanker@bub.ernet.in (G. Shanker), gurumurthy.hegde@christuniversity.in, murthyhegde@gmail.com (G. Hegde).
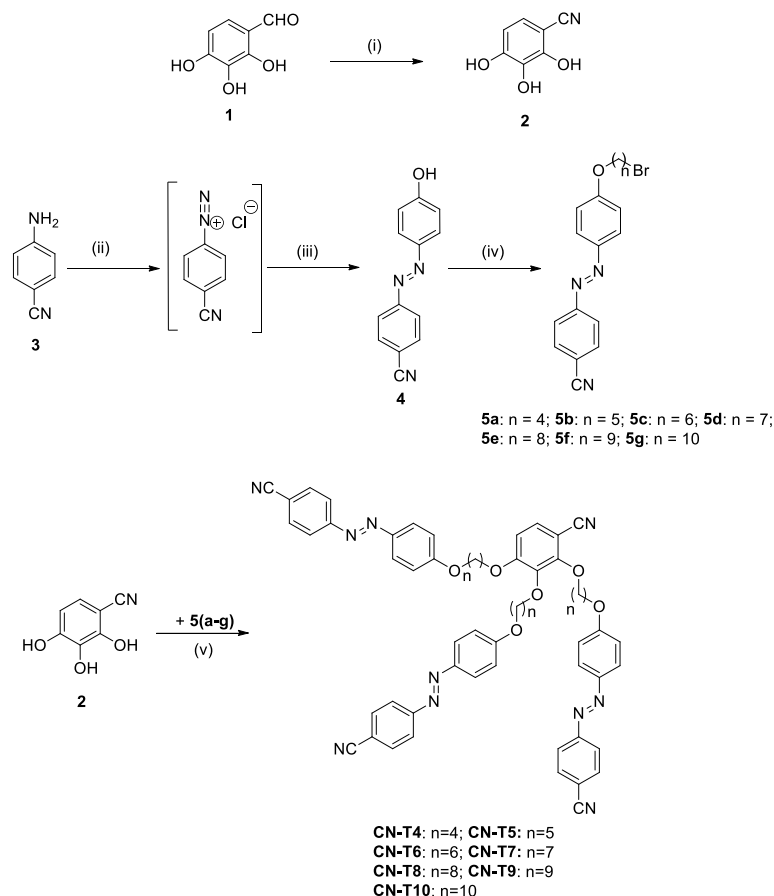
Reagents and conditions
(i) NH$_2$OH.HCl, dimethyl sulfoxide, reflux, 1 h, 90 °C, (85-92%).
(ii) NaNO$_2$, HCl, 0 to 5 °C.
(iii) 10% NaOH, Phenol, 0 °C, (80-85%).
(iv) K$_2$CO$_3$, KI (cat), butanone, reflux, N$_2$ atmosphere, 4 h, 80-92%.
(v) K$_2$CO$_3$, KI (cat), butanone, reflux, N$_2$ atmosphere, 48 h, 75-80%.

Scheme 1. Synthesis of trimers CN-Tn (n = 4 to 10).

[20–24] The photophysical behavior of trimers are entirely different from that of conventional calamitics and discotics LC materials, glassy phases are seen like in polymers [25–29]. Selection of proper segments towards the development of innovative thermotropic LC materials are important for advanced optoelectronics [30,31]. Our main perspective is to develop functionalized single component LCs with high sensitivity having multiple azo linkers, especially for the optical storage devices [32]. The azobenzene derivatives are photochemical chromophores exhibiting photo induced *cis-trans* isomerization, a perquisite criteria qualifies them as a good candidate for optoelectronic applications [33,34]. The azobenzene segment exhibit symmetrically allowed π-π* transition when irradiated with UV light λ ≈ 320 nm having molar absorptivity (ε > 1000 L mol-1 cm-1) and enters into *trans* state. The same moiety exhibits symmetrically forbidden n-π* transition when irradiated with visible light λ ≈ 450 nm having ε < 1000 L mol-1 cm-1, and attains *cis* isomer [35]. Reduced molecular symmetry is a promising approach for achieving low melting or room temperature liquid crystals [36–39] and is essential for photoresponsive behavior with substituted 1,2-diphenyldiazenyl groups [40,41]. In this study, we synthesized compounds by covalently linking 2,3,4-trihydroxybenzonitrile with substituted 1,2-diphenyldiazenyl units using flexible spacers. We then evaluated their thermal and photophysical properties. The shuttlecock-like geometry of these compounds makes their interaction with light particularly interesting to investigate. Additionally, the presence of three azo groups in the trimer suggests that intriguing DFT studies will be conducted in the near future [42,43].

2. Experimental

2.1. Synthesis

AR grade chemicals used as starting materials obtained from commercial sources, all solvents dried when necessary using standard procedure. The synthesis of substituted trimer bearing 4-((4-hydroxyphenyl)diazenyl)benzonitrile described in Scheme 1. NMR spectra (Fig. S1) and their data are furnished in ESI. The molecular structural characterisation of the materials confirmed using on ^{1}H and ^{13}C NMR (Varian Unity 500 and Varian Unity 400 spectrometers, in CDCl$_3$ solutions, with tetramethylsilane as internal standard). Microanalyses were performed using a Leco CHNS-932 elemental analyser.

The mesophase behaviour and transition temperatures of the trimers were measured using a Mettler FP-82 HT hot stage and control unit in conjunction with a Leica DM2700P polarising microscope. The associated enthalpies were obtained from DSC-thermograms, which were recorded on a PerkinElmer DSC-7, heating and cooling rate: 10 °C min^{-1}.

2.2. Synthesis of 2,3,4-trihydroxy benzonitrile (2) from commercially available 2,3,4-trihydroxy benzaldehyde

2,3,4-trihydroxy benzaldehyde (6.49 mmol, 1.0 equiv), NH$_2$OH.HCl (9.73 mmol, 1.5 equiv) in DMSO and refluxed at 90 °C for 1 h and the completion of reaction was monitored by TLC. The entire reaction mixture was poured into ice cold water and extracted with ethyl acetate. The organic layer was washed with brine and dried over anhydrous sodium sulphate and concentrated to afford the pure light brown solid which was further purified by recrystallization from ethanol.

2.3. Synthesis of (E)-4-((4-hydroxyphenyl)diazenyl)benzonitrile (4)

Sodium nitrate (10.15 mmol, 1.2 equiv) is dissolved in minimum quantity of water. 4-Amino benzonitrile (8.46 mmol, 1 equiv) is dissolved in 3N HCl and stirred at 0–5 °C for 0.5 h followed by the dropwise addition of sodium nitrate solution at 0–5 °C to afford a clear solution. This clear solution was added to the phenol (9.31 mmol, 1.1 equiv) dissolved in 10 % NaOH at 0–5 °C. Then reaction is stirred for 1 h. The pH of the solution was maintained at 4.5–5.0 by addition 1.5N HCl dropwise to afford orange colour precipitate. The solid so obtained was filtered and dried in vacuum.

2.4. Synthesis of (E)-4-((4-((n-bromoalkyl)oxy)phenyl)diazenyl)benzonitrile (5a-g)

A mixture of (E)-4-((4-hydroxyphenyl)diazenyl)benzonitrile (4.48 mmol, 1.0 equiv), dibromo-alkanes (6.72 mmol, 1.5 equiv), potassium carbonate (4.93 mmol, 1.1 equiv) and potassium iodide (catalytic quantity) in 10 ml of butanone and refluxed for 5 h under dry nitrogen atmosphere and the completion of reaction was monitored by TLC. The reaction mixture was cooled to room temperature and filtered over Celite bed with DCM and concentrated. The crude product so obtained was subjected to purification by column chromatography using neutral alumina. The column was eluted with 3 % EtOAc-hexane to afford pure orange color solid.

2.5. Synthesis of 2,3,4-tris[n-((4-(-cyanophenyl)diazenyl)phenoxy)alkyloxy]benzonitrile (CN-T4 to CN-T10)

A mixture of 2,3,4-trihydroxybenzonitrile (0.66 mmol, 1.0 equiv), ((E)-4-((n-bromoalkyl)oxy)phenyl)diazenyl)benzonitrile (1.985 mmol, 3.0 equiv), potassium carbonate (1.985 mmol, 3 equiv.) and potassium iodide (catalytic amount) in 10 ml of butanone and refluxed for 14 h under dry nitrogen atmosphere and completion of reaction was monitored by TLC. The reaction mixture was cooled to room temperature and filtered over Celite bed with DCM and concentrated. The crude product so obtained was subjected to purification by column chromatography using neutral alumina as stationary phase and DCM as eluent.

2.6. Photoisomerization studies

The photoisomerization studies were conducted using Ocean Optics HR 2000+ spectrophotometer, and absorption spectra were recorded. The photoconversion efficiency of *trans-cis* photoisomerization and the kinetics of *cis-trans* isomerization through thermal back relaxation were studied in solutions and solid states. The studies were conducted in the dark at room temperature (30 ± 1 °C). The solutions in chloroform were taken in a 1 cm quartz cuvette and covered to avoid the evaporation of the solvent. The spectral data for all the compounds were normalized for comparison. The solution under study was irradiated with UV light of 1 mW/cm^2 using an OMNICURE light source. A heat filter is inserted between the sample and the source to avoid the influence of UV heat on the sample. The absorption spectra of the compounds were investigated before and after UV illumination at varying intervals of time [44,45].

3. Results and discussion

3.1. Thermal behavior

The LC behavior of trimers **CN-T*n*** compounds characterized using polarizing optical microscope (POM), and differential scanning calorimeter (DSC). The samples were investigated under POM using untreated glass slides and the thermopeaks recorded in DSC thermograms, the phase transitions of all the compounds were consistent with those of the optical observations. LC phase transition

Table 1
Phase transition temperatures[a] (°C) and corresponding enthalpies (ΔH) [kJ mol^{-1}] of **CN-Tn** series. Cr = Crystal, N = Nematic, Iso = Isotropic.

Trimer	Spacer Length	Heating	T$_{Cr}$
CN-T4	n = 4	Cr 44 [3.4] N 202 [1.1] Iso	<20
CN-T5	n = 5	Cr 136 [55.1] N 146 [0.41] Iso	<20
CN-T6	n = 6	Cr 112 [14.3] N 164 [2.1] Iso	<20
CN-T7	n = 7	Cr 162 [33.6] N 164 [1.4] Iso	<20
CN-T8	n = 8	Cr 202 [57.0] N 207 [1.1] Iso	<20
CN-T9	n = 9	Cr 101 [48.2] N 161 [4.1] Iso	27
CN-T10	n = 10	Cr 105 [102.3] N 152 [4.7] Iso	24

temperatures obtained from the first and second heating of DSC thermograms scanned at a rate of 10 °C/min are tabulated in Table 1.

Table 1 and Fig. 1 are the compilation data POM, DSC data, all the trimers display enantiotropic N phase, homologues **CN-T4** to **CN-T8** exhibit super-cooled N phase below the room temperature without any crystallization (Fig. 1). CN-T6 trimer sandwiched between two ordinary glass slides and recorded its texture during cooling cycle, a slow growth of Schileren texture of nematic phase with source of light being perpendicular to the sample. A clear two and four brush pattern defect observed, on mechanical shear a thread like nematic texture with surface disclination line witnessed (see Fig. 2a and b). It is difficult to correlate the N phase behaviour within the trimer series, as the higher homologues does not exhibit super-cooled N phase. The microscopic texture of the remaining trimer resembles to **CN-T6** and their textures are furnished in ESI.

3.2. Aggregation studies

Aggregational behavior of these shuttle-cock shaped trimers are evaluated for their intermolecular interaction in the solution phase. UV–visible absorption spectra recorded for the trimers (**CN-Tn**) as a function of concentration in chloroform (CHCl$_3$). A maximum absorption at λ = 362 nm of 6 μm observed for **CN-T6** trimer, the intensity of peak decreases with dilution of concentration and finally breaks down below 0.39 μM, with 4 times less the intensity. A clear broad peaks suggests a strong intermolecular interactions arising mainly due to the diazo chromophore exhibits π—π* (symmetry allowed) and n—π* (symmetry forbidden) transitions. The noticeable peak with increased intensity in the B-band region around λ = 362 is due to high energy second π—π* transition (hypsochromic shift) as H aggregates (Fig. 3 inset). The peak shape remains the same with decrease in the intensity, a drastic

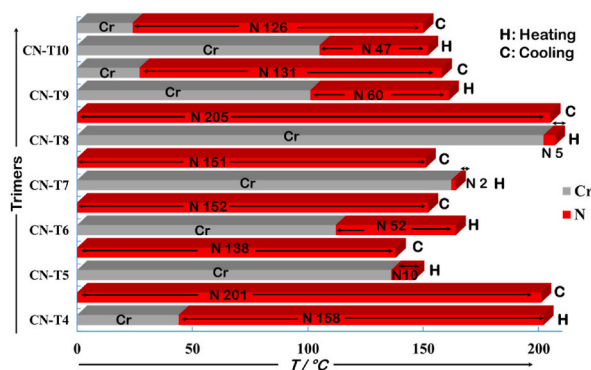**Fig. 1.** Bar diagram displaying the Cr and N phase transition of the trimers (**CN-Tn**) in both heating and cooling cycles scanned at the rate of 10 °C min^{-1}.
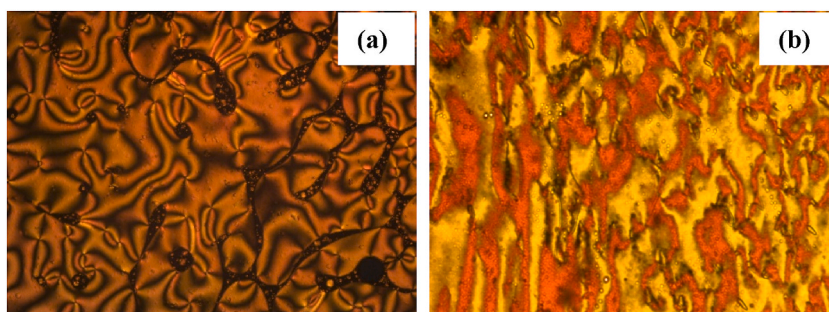

Fig. 2. Optical polarizing microscopic textures of trimer **CN-T6** (a) at 145 °C, (b) at 120 °C.
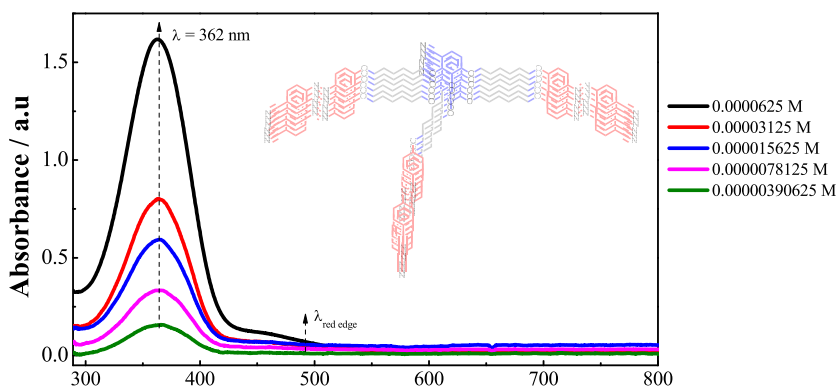
Fig. 3. Absorption spectra of **CN-T6** in CHCl$_3$ as a function of concentration, schematic representation of *H* aggregates (inset).

Table 2
Molar absorptivity of trimers as a function of concentration.

Trimers (µM)	Molar absorptivity (ε) (Lmol^{-1} cm^{-1})						
	CN-T4 (n = 4)	CN-T5 (n = 5)	CN-T6 (n = 6)	CN-T7 (n = 7)	CN-T8 (n = 8)	CN-T9 (n = 9)	CN-T10 (n = 10)
0.625	2.94×10^4	3.06×10^4	2.59×10^4	2.77×10^4	3.01×10^4	2.64×10^4	2.31×10^4
0.3125	3.40×10^4	3.40×10^4	2.60×10^4	2.78×10^4	3.08×10^4	2.85×10^4	2.62×10^4
0.15625	3.68×10^4	5.07×10^4	3.74×10^4	2.90×10^4	4.84×10^4	3.42×10^4	2.69×10^4
0.078125	4.62×10^4	6.11×10^4	3.94×10^4	3.08×10^4	5.02×10^4	3.59×10^4	3.37×10^4
0.0390625	5.78×10^4	7.66×10^4	4.09×10^4	3.76×10^4	6.02×10^4	4.27×10^4	4.01×10^4

Table 3
Data of *trans* to *cis* and *cis* to *trans* photoswitching time with respect to varying spacer length and their respective photoconversion efficiency.

Trimers	Spacer length	*trans* to *cis* photo-switching time (sec)	*cis* to *trans* back relaxation time (min)	PCE (%)
CN-T4	n = 4	50	318	86
CN-T5	n = 5	50	450	86
CN-T6	n = 6	50	400	85
CN-T7	n = 7	50	610	88
CN-T8	n = 8	50	620	86
CN-T9	n = 9	50	408	84
CN-T10	n = 10	40	558	86

aggregational change observed between 6 and 0.39 µM with 9.5 times lower intensity. A constant decrease in intensity observed between 3.1, 1.5, and 0.78 µM, which emphasizes on the aggregate size, the molar absorbance. A clear relation between the absorbance and concentrations are observed for all the trimers, molar absorptivity (ε) calculated using the equation $\varepsilon = A/lc$, where in A = absorbance, l = path length, c = concentration, results are tabulated in Table 2, as the concentration decreases the molar absorptivity increases due to the influence factors like amount of light absorbed by the trimer for specific wavelength, distance of light travel through the solution, concentration of absorbance per unit volume (See ESI, Fig. S3) (see Table 3).

3.3. Photoisomerization studies in solution

The photoisomerization properties of the triazo compounds with varying chain length were studied before and after UV illumination. All compounds were observed to have a prominent absorption band between 362 and 366 nm and a relatively weak absorption band around 450 nm before UV illumination. The prominent band corresponds to the symmetry allowed π—π* transition and the latter relatively weak band is due to the symmetry forbidden n—π* transition.

With UV illumination, the absorption peak due to the π—π* transition gradually decreased due to *trans*—*cis* conversion, and a slight increase in the absorption peak at 450 nm occurred, corresponding to the n—π* transition. This outcome is due to the photochromic characteristic of the azo group. Fig. 4 demonstrates the spectral changes of the compounds during UV exposure.

All compounds exhibited photoconversion efficiencies of more than 85 % after exposure to UV light at 365 nm. PCE, the extent of photoisomerization, was calculated using Equation (1).
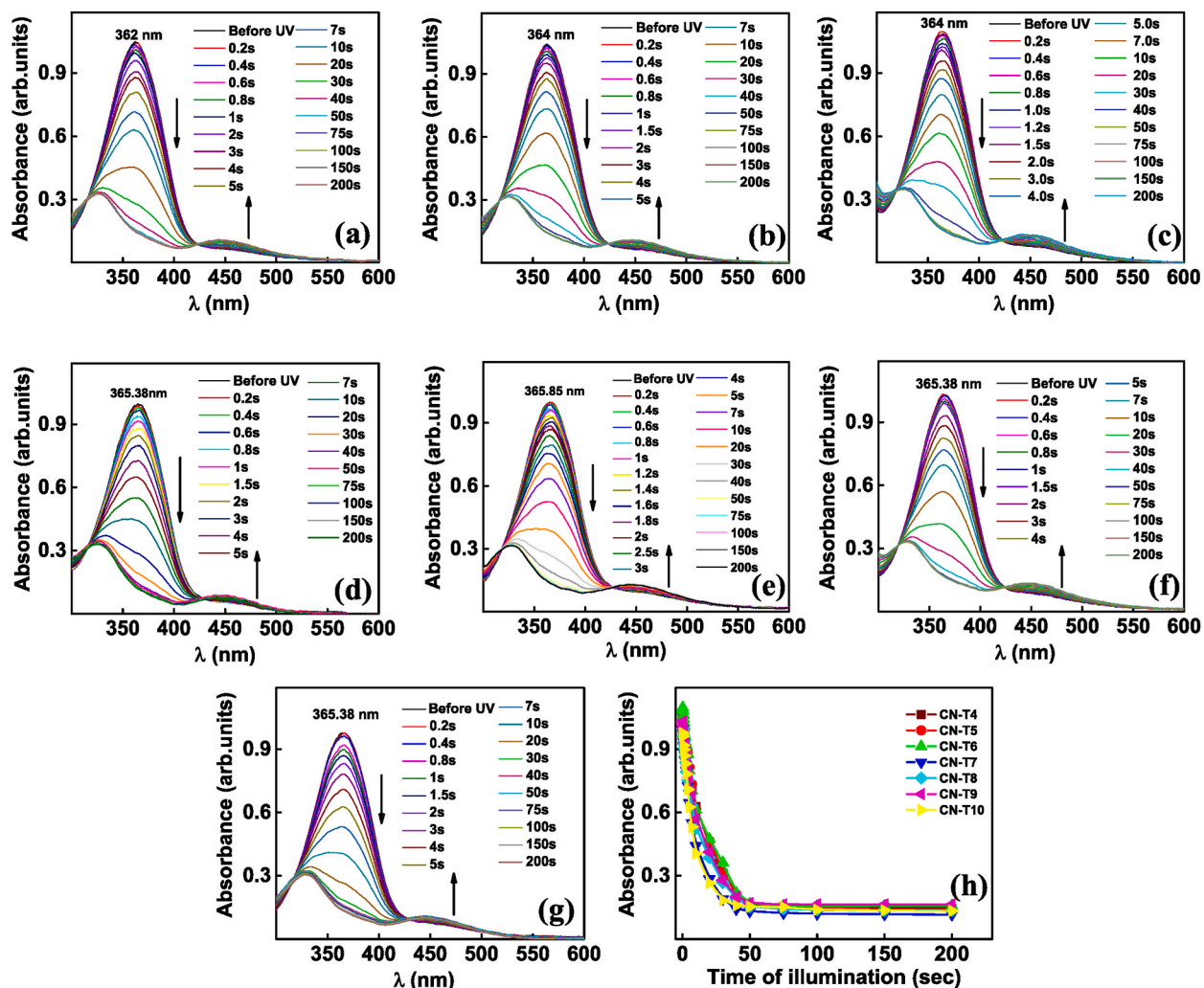
Fig. 4. Spectral changes brought about by UV exposure (a) **CN-T4**, (b) **CN-T5**, (c) **CN-T6**, (d) **CN-T7**, (e) **CN-T8**, (f) **CN-T9**, (g) **CN-T10**, (h) The plot of peak absorbance Vs. time of illumination. All the trimers photo-saturates at around 50 s.

$$PCE = \frac{A(t_0) - A(t_\infty)}{A(t_0)} \times 100 \tag{1}$$

here $A(t_0)$ is the initial absorbance (before UV exposure) and $A(t_\infty)$ is the final absorbance (after UV exposure).

Allowing the solution in the dark after UV irradiation leads to thermal back relaxation, causing a reversal from *cis* to *trans*. The system can be restored to its original position by exposing it to approximately 450 nm wavelength white light. Our study focuses solely on thermal back relaxation and its impact on the molecule's structure. Fig. 5 demonstrates the spectral changes during this process. **CN-T8** exhibits the longest thermal back relaxation time compared to other compounds.

3.4. Photoisomerization kinetics

The first order plot for *trans-cis-trans* photoisomerization is measured using Equation 2

$$ln\frac{A_\infty - A_t}{A_\infty - A_0} = -k_{C-t}t \tag{2}$$

where A_0, A_t, A_∞ are the absorbance values at peak maximum wavelength initial time (zero), time t, and an infinity time respectively. Fig. 6 illustrates the first-order plot for the compounds. The compounds initially follow first-order kinetics, but subsequently deviated from the curve due to a prolonged thermal back relaxation period that may have influenced the temperature conditions in the experiment.
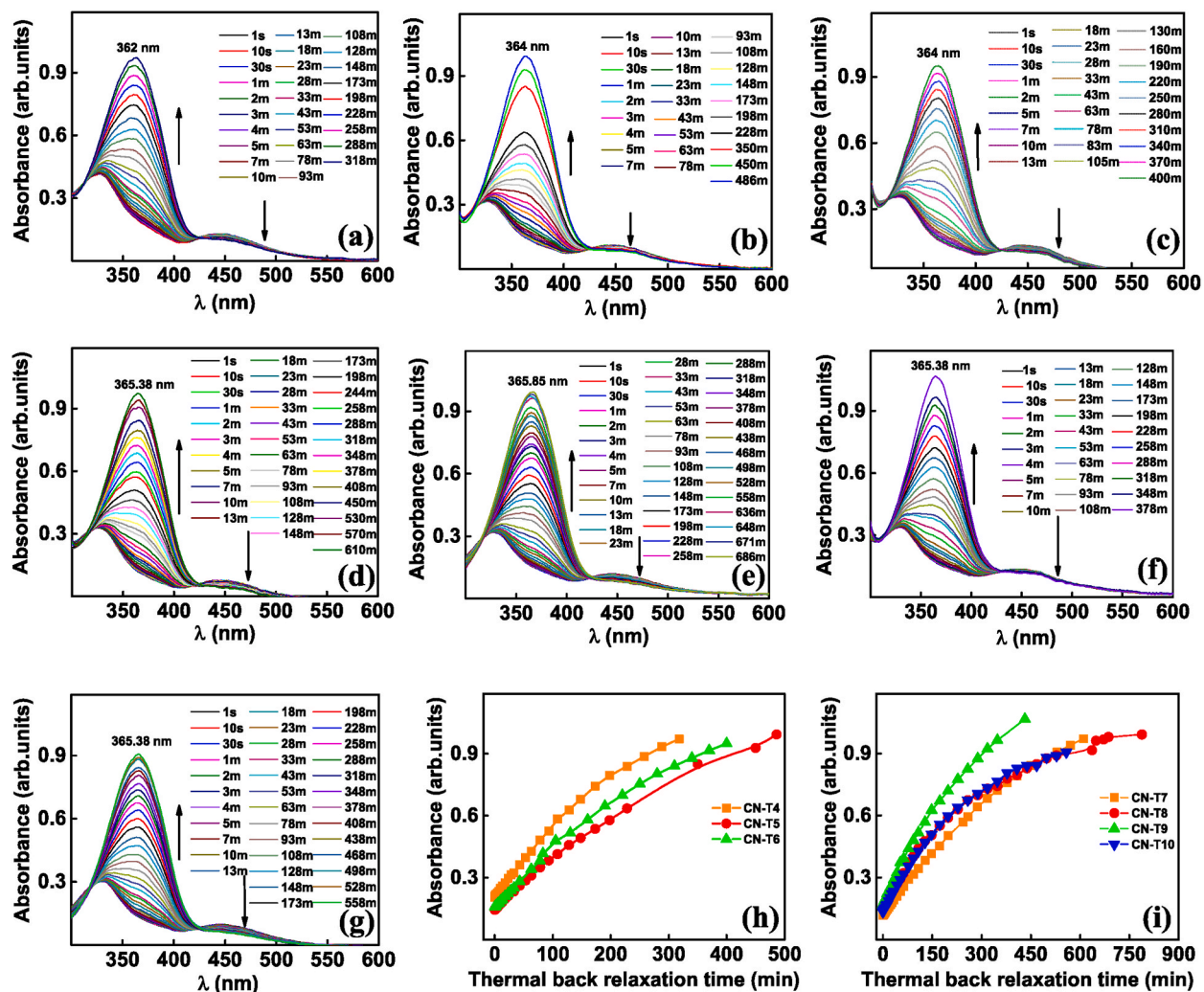
Fig. 5. Changes in the absorption spectra during thermal back relaxation (a) **CN-T4**, (b) **CN-T5**, (c) **CN-T6**, (d) **CN-T7**, (e) **CN-T8**, (f) **CN-T9**, (g) **CN-T10**, (h) & (i) The plot of peak absorbance Vs. thermal back relaxation time of a, b, c, d, e, f and g.
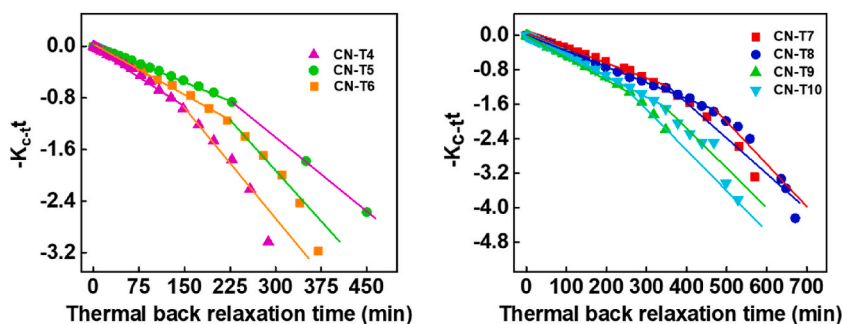

Fig. 6. First-order plot of the investigated compounds as a function of time for *cis-trans*.

3.5. Reason behind the phenomena

Although it is difficult to predict the exact reason behind the phenomenon, both in solutions and in solids, we attempt to explain it using a model known as the shuttlecock model. If one closely observes the chemical structure, it resembles a shuttlecock to the naked eye. We have used this model to explain the phenomenon to the best of our ability. Two main types can be considered here, namely, in
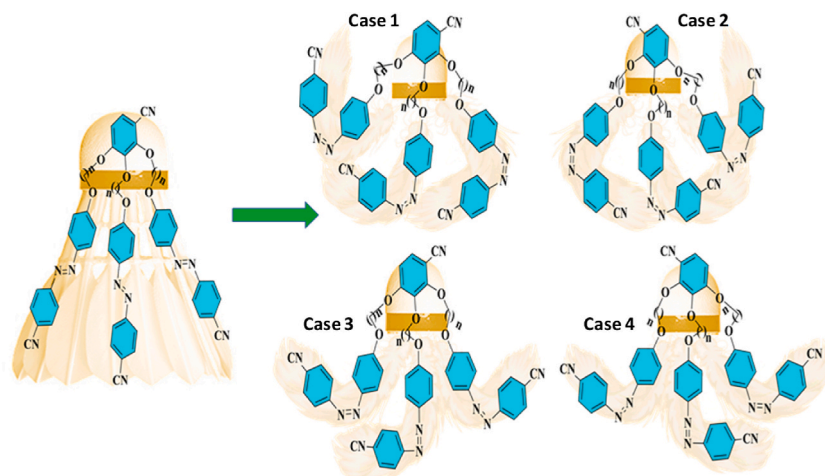
Fig. 7. Graphical representation of photoisomerization of trimers with UV illumination using shuttle cock model in solutions. One can observe that, when light of 365 nm UV is shined on the said materials, four cases might appear. Case 1 and 2, where azobenzene arms may distort at the same side, case 3 and 4, two of the azobenzene arms distort in one side and another bend to their opposite side.
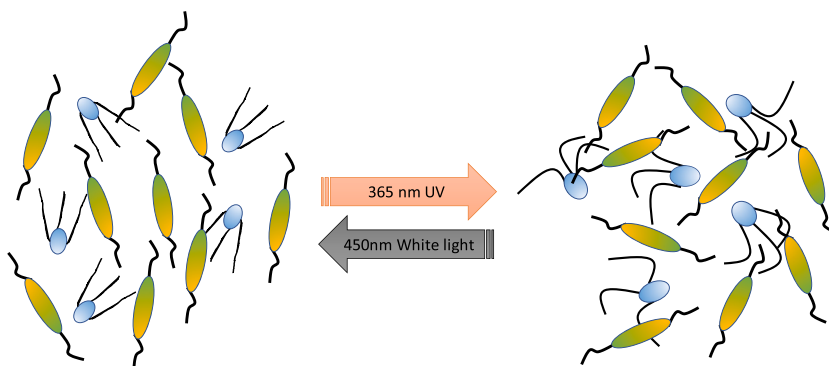

Fig. 8. Graphical representation of photoisomerization of guest-host system. One can observe that, when light of 365 nm UV is shined on the said materials, energetically stable liquid crystals (left side) changed to metastable *cis* configuration whereas shuttle cock shaped trimers converted to distorted shuttle cock structure (right side).

solutions and in solids.

3.5.1. System in solution (only azobenzene molecules in to consideration)

We observed during UV spectroscopy measurements that all the said compounds have a fast photo-switching time. This is mainly because the UV experiments are intensity-controlled, allowing us to tune the photo-switching time. However, when the UV light is switched off, the process becomes entirely temperature-driven, resulting in different thermal back relaxation times for different molecules, depending entirely on their chemical structures. Based on this observation, we can conclude that **CN-T7, CN-T8**, and **CN-T10** are long thermal back relaxation materials, whereas **CN-T4** and **CN-T6** are fast-relaxing materials in that series. Interestingly, all these trimers show more than 5 h of thermal back relaxation.

It is evident from Fig. 7, that considering the times as shuttlecock shaped before illumination, four cases may be possible after UV light illumination. In any case, we will obtain a distorted shuttlecock structure due to the bending of the azobenzenes.

Case 1 & 2. After 365 nm UV illumination, all three azobenzene arms might bend on the same side (either right or left bending). Due to this, molecules like **CN-T4, CN-T5, CN-T6**, and **CN-T9** might relax a little faster than their counterparts since the distortion is less aggressive compared to case 3 and case 4.

Case 3 & 4. After UV illumination, two arms bend in one direction, and another bend in the opposite direction. This, creates many difficulties for the molecules to relax. In such cases, molecules like **CN-T7**, **CN-T8**, and **CN-T10** take longer to relax. Additionally, such structures have more flexibility compared to their counterparts.
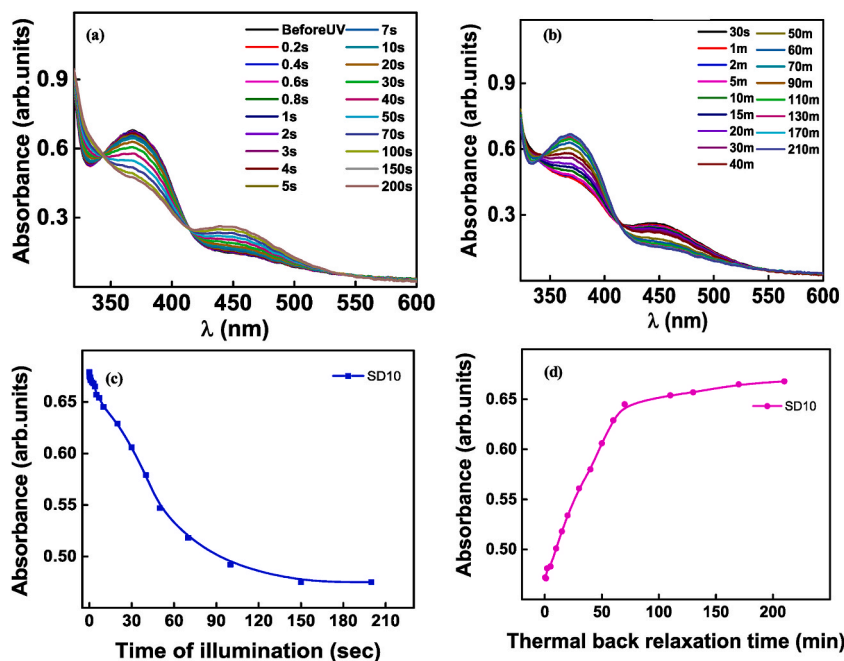
Fig. 9. Effect of light on guest-host effect based liquid crystalline cells where UV ON taking place around 120 s (see a and c) and UV OFF takes around 3 h (b and d) showing the potential of the material to use as optical storage devices. UV intensity used is 1 mW/cm^2.
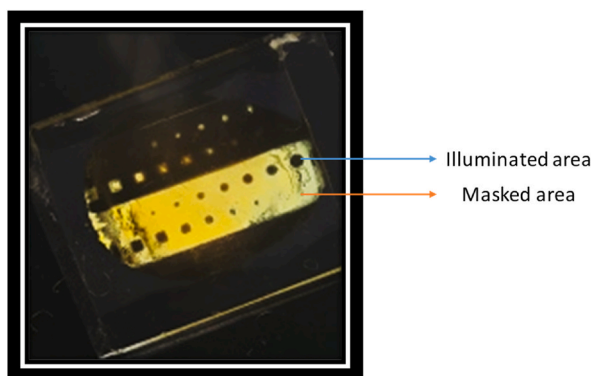

Fig. 10. Optical storage device constructed using the **CN-T10** along with 5CB, room temperature liquid crystals. Illuminated area showing dark state due to isotropic region under the crossed polarizers whereas masked region shows nematic state. UV intensity used is 5 mW/cm^2 and illumination is 5 min.

3.5.2. System is in solid state (guest-host mixture form)

When we add 5 % of the guest azobenzene (**CN-T10**) with the 95 % host liquid crystalline (5CB) system, azobenzene molecules will bend due to *trans-cis* configuration. In contrast, liquid crystal molecules randomly align due to their isotropic state attainment. Initially, liquid crystals and trimers are in a favorable condition (as shown in Fig. 8 left). As soon as 365 nm UV light is shone on them, trimers change their structure entirely and appear as a distorted shuttlecock. Host liquid crystals (5CB) change from a nematic order state to a disordered isotropic state. When the lights are turned off, the entire system becomes complicated (see Fig. 8 right), and due to this, liquid crystal molecules take longer to travel from the isotropic state to the ordered state. Because of this, we get a long thermal back relaxation in such trimers.

3.6. Photoisomerization studies in solids

Soft matter is expected to be an intrinsic part of the next generation of advanced devices and digitally augmented technologies [46]. Soft materials such as gels, polymers, liquid crystals, and biological materials enriched with photo-responsiveness have recently emerged as multifunctional advanced optical materials for diverse applications [47,48]. In this regard, liquid crystals (LCs) exhibiting

photoresponsive behavior and adaptive attributes could serve as promising innovative soft materials. Studying optical storage devices is crucial from a commercialization point of view. For the devices, guest trimer **CN-T10**, which has higher thermal back relaxation and long-range nematics, was used along with host liquid crystalline molecules 5CB. 5 % of the guest was mixed with 95 % of the host, and the mixture was capillary-filled inside the previously prepared ITO-coated cells. UV light of wavelength 365 nm was shined on them at subsequent intervals, and the UV spectra were captured (see Fig. 9a and c). Similarly, thermal back relaxation spectra were recorded by turning off the UV light (see Fig. 9b and d).

The UV intensity used is 1 mW/cm^2, and a heat filter is used between the sample and the light source to eliminate any heating effects. One can see that the photo-switching time is around 120 s, whereas the back relaxation time is around 3 h, showing the potential of the materials.

3.7. Optical storage device

An optical storage device is constructed using the above-mentioned procedure, and a suitable mask is placed above the liquid crystal cells, which were previously filled with 5 % of the guest material (**CN-T10**) and 95 % of the host material (5CB). A UV intensity of 5 mW/cm^2 is applied for 5 min. As can be seen from Fig. 10, the UV-illuminated area transforms to a dark state (disordered state).

The birefringent nematic state remained bright, while the masked state turned dark, highlighting the trimers' potential for optical storage devices.

4. Conclusions

We synthesized and characterized shuttlecock-shaped trimers to explore their thermal and liquid crystalline behaviors. All the trimers, except for the two higher homologues, displayed a super-cooled nematic phase. In the UV–Visible absorption spectra, all the trimers with H-aggregated structures exhibited a strong B-band at $\lambda_{max} = 362$ nm, with a calculated band gap ranging from 2.3 to 2.4 eV. **CN-T10** stood out with its rapid photo-switching from cis to trans isomer, achieving an impressive 86 % photo-conversion efficiency and demonstrating prolonged thermal back relaxation of approximately 10 h, showcasing its potential as an optical storage device. These findings underscore the significant impact of light as an external stimulus on the structure-property relationships of these materials. Cost-effective and easy to synthesize, these trimers open up promising new directions for the development of liquid crystalline materials. This study does not include the use of photo cross-linkers, which could potentially restrict thermal back relaxation of the molecules and enhance their optical storage properties. Exploring this aspect could be valuable in future research.

CRediT authorship contribution statement

D. Sandhya Kumari: Investigation, Formal analysis. **Apoorva Shetty:** Methodology, Investigation, Formal analysis. **B.S. Ranjitha:** Methodology, Investigation, Formal analysis. **Vandana M:** Validation, Methodology, Investigation. **G. Shanker:** Writing – review & editing, Writing – original draft, Validation, Supervision, Conceptualization. **Mohamed Alaasar:** Writing – review & editing, Validation, Conceptualization. **Gurumurthy Hegde:** Writing – review & editing, Supervision, Methodology, Investigation, Conceptualization.

Declaration of competing interest

The authors declare that they have no known competing financial interests or personal relationships that could have appeared to influence the work reported in this paper.

Appendix A. Supplementary data

Supplementary data to this article can be found online at https://doi.org/10.1016/j.heliyon.2024.e37455.

References

[1] H.K. Bisoyi, Q. Li, Chem. Rev. 5 (2022) 4887–4926.
[2] M. Goh, S.M.K. Akagi, Chem. Soc. Rev. 39 (2010) 2466–2476.
[3] R.J. Bushby, K. Kawata, Liq. Cryst. 38 (2011) 1415.
[4] Takashi Kato, Junya Uchida, Takahiro Ichikawa, Takeshi Sakamoto, Angew. Chem. Int. Ed. 57 (2018) 2–19.

[5] J.A. Castellano, Singapore: World Scientific, 2005.
[6] Shanker Govindaswamy, K.R. Sunil Kumar, Bishwajit Paul, Liq. Cryst. 49 (12) (2022) 1545–1603.
[7] J.W. Goodby, P.J. Collings, T. Kato T, Weinheim: Wiley-VCH, 2014.
[8] G. Shanker, B. Paul, A. Ganjiwale, Curr. Org. Synth. 18 (2021) 333–351.
[9] C.V. Yelamaggad, G. Shanker, U.S. Hiremath, J. Mater. Chem. 18 (2008) 2927–2949.
[10] G.W. Gray, London and New York: Academic Press, Inc, 1962.
[11] A.S. Achalkumar, U.S. Hiremath, D.S. Shankar Rao, C.V. Yelamaggad, Liq. Cryst. 38 (2011) 1563–1589.
[12] A. Miniewicz, J. Girones, P. Karpinski, B. Mossety-Leszczak, H. Galina, M. Dutkiewicz, J. Mater. Chem. C 2 (2014) 432.
[13] N.A. Razali, Z. Jamain, Polymers (13) (2021) 3462.
[14] B.D. Zielinska, D. Szmigiel, A. Kysil, O. Krupka, A.K. Szmigiel, J. Phys. Chem. C 124 (2020) 939–944.
[15] H.A. Sultan, A.M. Dhumad, Q.M.A. Hassan, T. Fahad, C.A. Emshary, N.A. Raheem, Spectrochim. Acta Mol. Biomol. Spectrosc. 251 (2021) 119487.
[16] H. Yu, J. Mater. Chem. C (2) (2014) 3047–3054.
[17] R.S. Hegde, B.N. Sunil, G. Hegde, V. Prasad, J. Mol. Liq. (309) (2020) 113091.
[18] H. Li, J. Wang, C. Wang, P. Zeng, P. Cai, Y. Pan, Y. Yang, Opt. Mater. Express (6) (2016) 460.
[19] G.W. Gray, Mol. Cryst. 7 (1969) 127–151.
[20] Michal Smahel Shruthi, Michal Kohout, G. Shanker, Gurumurthy Hegde, J. Mol. Liq. 339 (10) (2021) 116744.
[21] B.N. Sunil, M.K. Srinatha, G. Shanker, Gurumurthy Hegde, M. Alaasard, C. Tschierske, J. Mol. Liq. 304 (2020) 112719.
[22] Gurumurthy Hegde, G. Shanker, S.M. Gan, A.R. Yuvaraj, Syed Mahmood, Uttam Kumar Mandal, Liq. Cryst. 11 (2016) 1578–1588.
[23] B. N Sunil, M. Monika, G. Shanker, Gurumurthy Hegde, Veena Prasad, Evaluation of photo switching properties for hockey stick - shaped mesogens bearing azo benzene moieties, Frontiers in Physics 9 (2021) 728632, 1-9.
[24] B.S. Ranjitha, D. Sandhya Kumari, Apoorva Shetty, G. Shanker, Mohamed Alaasar, Rami Pashameah, Gurumurthy Hegde, J. Mol. Liq. 383 (2023) 121985.
[25] W.E. Lee, C.L. Lee, T. Sakaguchi, M. Fujiki, G. Kwak, Chem. Commun. 47 (2011) 3526.
[26] H. Hayashi, T. Iseki, S. Nimori, H. Goto, Sci. Rep. 7 (2017) 3948.
[27] A.M. Donald, A.H. Windle, Cambridge University Press, Cambridge, 1992.
[28] R.L. Kerr, S.A. Miller, R.K. Shoemaker, B.J. Elliott, D.L. Gin, J. Am. Chem. Soc. 131 (2009) 15972.
[29] D.G. Kim, Y.H. Kim, T.J. Shin, E.J. Cha, D.S. Kim, B.G. Kim, Y. Yoo, Y.S. Kim, M.H. Yi, J.C. Won, Chem. Commun. 53 (2017) 8227.
[30] T. Kato, N. Mizoshita, K. Kishimoto, Angew. Chem. Int. 45 (44) (2006) 118.
[31] T. Kato, Struct. Bonding (Berlin) 96 (2000) 95.
[32] J. Henzl, M. Mehlhorn, H. Gawronski, K.H. Rieder, K. Morgenstern, Angew. Chem. Int. Ed. 45 (2006) 603–606.
[33] X. Wang, Z. Li, H. Zhao, S. Chen, R. Soc. Open Sci. 7 (2020) 200474.
[34] A. Cembran, F. Bernardi, M. Garavelli, L. Gagliardi, G. Orlandi, J. Am. Chem. Soc. 126 (2004) 3234–3243.
[35] W.C. Xu, S. Sun, S. Wu, Angew. Chem. Int. Ed. (2019) 14441.
[36] G. Shanker, M.K. Srinatha, Ocak Hale, Liq. Cryst. 50 (2) (2022) 1–8.
[37] M.K. Srinatha, Ayesha Zeba, Anjali Ganjiwale, Ashwathanarayana Gowda, Gurumurthy Hegde, Alaasar Mohamed, G. Shanker, Liq. Cryst. 49 (2021) 217–229.
[38] M.K. Srinatha, S. Poppe, G. Shanker, M. Alaasar, C. Tschierske, J. Mol. Liq. 317 (2020) 114244.
[39] G. Shanker, A. Bindushree, K. Chaithra, P. Pratap, Ravindra Kumar Gupta, A.S. Achalkumar, C.V. Yelamaggad, J. Mol. Liq. 275 (2019) 849–858.
[40] S. Kurihara, K. Ohta, T. Oda, R. Izumi, Y. Kuwahara, T. Ogata, S.N. Kim, Sci. Rep. 3 (2013) 2167.
[41] T. Ikeda, O. Tsutsumi, Science 268 (1995) 1873–1875.
[42] S. Nada, M. Hagar, O. Farahat, A.A. Hasanein, A.-H. Emwas, A.A. Sharfalddin, M. Jaremko, M.A. Zakaria, Molecules 27 (2022) 2304.
[43] M.A. Zakaria, M. Alazmi, K.D. Katariya, Y. El Kilany, E.S.H. El Ashry, M. Jaremko, M. Hagar, S.Z. Mohammady, Crystals 11 (2021) 978.
[44] E. Merino, M. Ribagorda, Beilstein J. Org. Chem. (8) (2012) 1071–1090.
[45] X. Wang, Z. Li, H. Zhao, S. Chen, R. Soc. Open Sci. 7 (2020) 200474.
[46] H.K. Bisoyi, Q. Li, Chem. Rev. 122 (2022) 4887–4926.
[47] Q. Li, A.P.H.J. Schenning, T.J. Bunning, Adv. Opt. Mater. 7 (2019) 1901160.
[48] G. Pathak, G. Hegde, V. Prasad, J. Mol. Liq. 314 (2020) 113643.